IEEE Photonics Journal
An IEEE Photonics Society Publication

Open Access

Engineering of AlGaN-Delta-GaN Quantum-Well Gain Media for Mid- and Deep-Ultraviolet Lasers

Volume 5, Number 2, April 2013

Jing Zhang, Student Member, IEEE
Nelson Tansu, Senior Member, IEEE

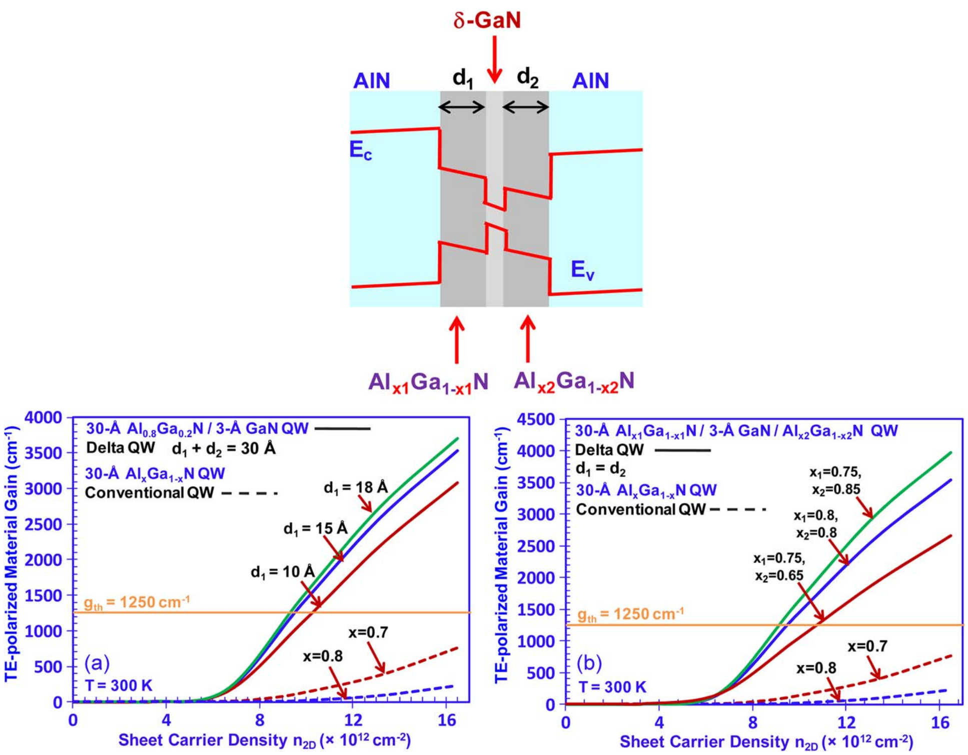

DOI: 10.1109/JPHOT.2013.2248705
1943-0655/$31.00 ©2013 IEEE

IEEE photonics SOCIETY
IEEE

Engineering of AlGaN-Delta-GaN Quantum-Well Gain Media for Mid- and Deep-Ultraviolet Lasers

Jing Zhang, ***Student Member, IEEE***, **and Nelson Tansu**, ***Senior Member, IEEE***

Center for Photonics and Nanoelectronics, Department of Electrical and Computer Engineering,
Lehigh University, Bethlehem, PA 18015 USA

DOI: 10.1109/JPHOT.2013.2248705

Manuscript received December 16, 2012; revised February 8, 2013; accepted February 14, 2013. Date of publication February 22, 2013; date of current version March 8, 2013. This work was supported in part by the U.S. National Science Foundation under Grants ECCS 0701421, DMR 0907260, and ECCS 1028490, and in part by the Class of 1961 Professorship Fund. The work was previously presented in SPIE Photonics West 2012 (San Francisco, CA, Jan. 2012). Corresponding author: J. Zhang and N. Tansu (e-mail: jiz209@Lehigh.Edu; Tansu@Lehigh.Edu).

Abstract: The gain characteristics of AlGaN-delta-GaN quantum wells (QWs) with varying delta-GaN positions and AlGaN QW compositions are analyzed. The use of optimized AlGaN-delta-GaN QWs resulted in $\sim$7-times increase in material gain over that of conventional AlGaN QWs for gain media emitting at $\sim$240 nm. By employing asymmetric AlGaN-delta-GaN QWs, the optimized optical gain can be achievable for AlGaN-delta-GaN QW structure with realistic design applicable for mid- and deep-ultraviolet (UV) lasers. The threshold properties and differential gains are also studied for optimized AlGaN-delta-GaN QWs UV lasers.

Index Terms: III-Nitride, AlGaN-delta-GaN quantum wells (QWs), deep UV (UV) lasers, optical gain, laser diodes.

1. Introduction

The field of III-Nitride semiconductors has applications covering lasers and light-emitting diodes (LEDs) [1]–[16], power electronics [17], thermoelectric [18], [19], photovoltaics [20], and terahertz photonics [21]. Significant advances had been achieved in visible LEDs, especially in addressing the internal quantum efficiency [1]–[4], material epitaxy [5]–[10], extraction efficiency [11], [12], and efficiency droop [13]–[16]. In contrast to the progress in visible emitters [1]–[16], the realization of electrically injected mid- ($\lambda \sim 250-320$ nm) and deep-ultraviolet (UV) ($\lambda \sim 220-250$ nm) AlGaN quantum wells (QWs) lasers has been limited to $\lambda \sim 320-360$ nm [22]–[39], while only optically pumped deep-UV lasers had been realized for shorter emission wavelength [31]. The challenges in realizing the electrically injected mid- and deep-UV AlGaN QWs lasers are attributed to the difficult growths of high Al-content AlGaN and p-AlN and the lack understanding on the physics of high Al-content AlGaN QWs. The optical properties for low [40]–[42] and high Al-content [43], [44] AlGaN QWs lasers have been reported, while the studies are relatively lacking on gain properties of high Al-content AlGaN QWs.

Our recent work [43] revealed the valence subbands crossover in high Al-content AlGaN QW leads to strong conduction (C)-crystal-field split-off hole (CH) transition, which results in large transverse-magnetic (TM)-polarized optical gain for $\lambda \sim 220-230$ nm. Recent experimental works have confirmed the dominant TM-polarized emission for shorter wavelength with higher Al-content

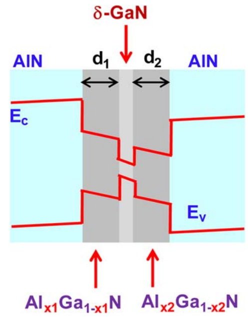

Fig. 1. Schematic energy band lineup of $Al_{x1}Ga_{1-x1}N$/delta-GaN/$Al_{x2}Ga_{1-x2}N$ QW with AlN barriers.

AlGaN QWs LEDs [45], [46], in agreement with our prediction [43]. The subsequent paper has studied about the temperature and barrier effect on the polarization properties of AlGaN QW [47]. Recent theoretical work [48] has confirmed the crossover of the valence subbands for AlGaN alloys on $Al_{0.85}Ga_{0.15}N$ substrate, in agreement with our finding [43]. The subsequent theoretical work [49] has discussed the strain effect by using various AlGaN substrates on the crossover in AlGaN. Garrett and coworkers have experimentally confirmed our prediction of the CH/HH crossover for AlGaN QWs from the transverse-electric (TE) ($\lambda \sim 253$ nm) to TM ($\lambda \sim 237$ nm) photoluminescence polarization switching [50].

In order to address the issue of low optical gain at $\lambda \sim 250-300$ nm, we recently proposed the AlGaN-delta-GaN QW structure [51] by inserting an ultrathin GaN layer into high Al-content (x) $Al_xGa_{1-x}N$-delta-GaN QW active region. The use of AlGaN-delta-GaN QWs resulted in strong valence subband mixing, which led to large TE-polarized gain at $\lambda \sim 240-300$ nm attributed to the dominant C–HH transition. Recent experimental work [52] has reported the polarization properties of the deep-UV emission from AlN/GaN short-period superlattices, which revealed that stronger TE-polarized emission from the use of a very thin GaN in AlN active region similar to our prediction [51]. Note that the use of InGaN-delta-InN QW had been used for achieving improved overlap design in visible LEDs [53], [54].

In this paper, we present a comprehensive study on the optical gain and threshold characteristics of AlGaN-delta-GaN QWs with various delta-GaN positions and AlGaN QW compositions for mid- and deep-UV lasers. The band structure and wave function calculations are based on the six-band $\boldsymbol{k} \cdot \boldsymbol{p}$ formalism for wurtzite semiconductors taking into account the valence band mixing, strain effect, polarization fields, and carrier screening effects [55]–[59], with the III-Nitride band parameters and band offsets ratio ($\Delta E_c/\Delta E_v = 70/30$) obtained from references [59]–[61]. The spontaneous and piezoelectric polarizations follow the treatments in [62] and [63], respectively.

2. Concept and Band Structure for AlGaN-Delta-GaN QWs

Fig. 1 shows the schematic of the AlGaN-delta-GaN QW. Our previous work [51] revealed that the use of symmetric high Al-content AlGaN-delta-GaN QWs led to large TE-polarized gain at $\lambda \sim 240-300$ nm. In this paper, we present a comprehensive study of the asymmetric AlGaN-delta-GaN QWs. The asymmetric QWs can be introduced by engineering the thicknesses of the AlGaN layers (d_1, d_2) and/or the Al contents of the AlGaN layers (x_1, x_2) surrounding the delta-GaN layer.

For the AlGaN-delta-GaN QWs, the energy levels of the HH and light hole (LH) subbands are higher than those of the CH subband, which leads to the dominant C–HH transition. The difference in the effective masses of the electrons and holes leads to different spreading of the wave functions for electrons and holes in III-Nitride-based QWs. In the case of identical effective masses for both electrons and holes, the optimized overlap will occur with the delta position at the center of the QWs. However, the effective masses for holes are larger than those of electrons in nitride-based QWs; thus, the optimization of the overlap can be achieved by using engineering of the delta layer

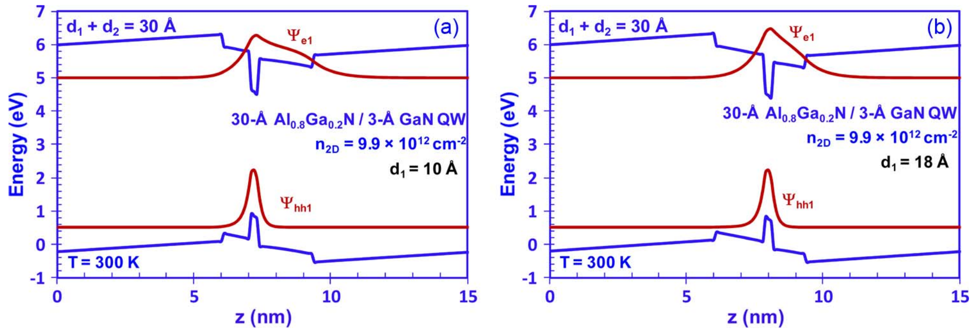

Fig. 2. Energy lineups with electron wavefunction EC1 and hole wave function HH1 for the 30-Å $Al_{0.8}Ga_{0.2}N$/3-Å GaN QW with (a) $d_1 = 10$ Å, and (b) $d_1 = 18$ Å.

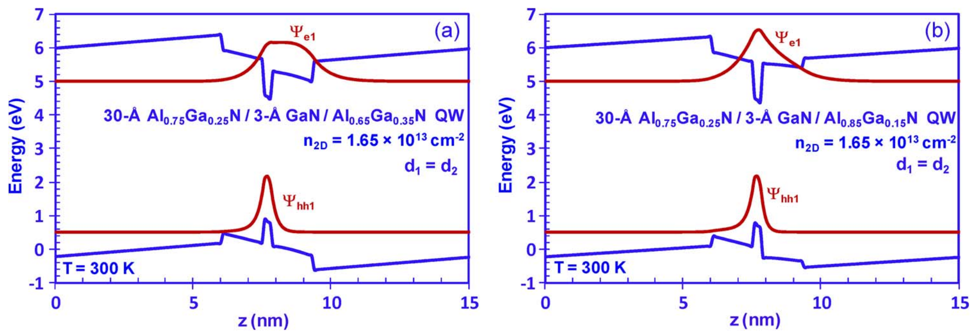

Fig. 3. Energy lineups with electron and hole wavefunctions for (a) the 30-Å $Al_{0.75}Ga_{0.25}N$/3-Å GaN/ $Al_{0.65}Ga_{0.35}N$ QW, and (b) the 30-Å $Al_{0.75}Ga_{0.25}N$/3-Å GaN/$Al_{0.85}Ga_{0.15}N$ QW.

position (d_1, d_2) [Fig. 2(a) and (b)] or different compositions of AlGaN QW sublayers (x_1, x_2) [see Fig. 3(a) and (b)].

Fig. 2(a) and (b) shows the energy lineups with electron wavefunction EC1 and hole wave function HH1 for the 30-Å $Al_{0.8}Ga_{0.2}N$/3-Å GaN QW with different d_1 thicknesses $(d_1 + d_2 = 30$ Å$)$ at the sheet carrier density (n_{2D}) of 9.9×10^{12} cm^{-2} (T = 300 K). For the 30-Å $Al_{0.8}Ga_{0.2}N$/3-Å GaN QW structure with $d_1 = 10$ Å in Fig. 2(a), the electron–hole wavefunction overlap (Γ_{e_hh}) is obtained as ~63.51%. By engineering the delta QW structure with $d_1 = 18$ Å, as shown in Fig. 2(b), the electron and hole wavefunctions are strongly localized toward the center of the QW active region, attributing to the engineered spreading of the wavefunctions, which leads to the enhanced $\Gamma_{e\_hh} \sim 73.92\%$.

Fig. 3(a) and (b) shows the energy band lineups with electron wavefunction EC1 and hole wave function HH1 for the 30-Å $Al_{0.75}Ga_{0.25}N$/3-Å GaN/$Al_{0.65}Ga_{0.35}N$ QW and $Al_{0.75}Ga_{0.25}N$/3-Å GaN/ $Al_{0.85}Ga_{0.15}N$ QW with $n_{2D} = 1.65 \times 10^{13}$ cm^{-2} at T = 300 K, and the thickness d_1 is kept as identical with the thickness d_2. For the 30-Å $Al_{0.75}Ga_{0.25}N$/3-Å GaN/$Al_{0.65}Ga_{0.35}N$ QW, the design consisting of asymmetric QW with different Al contents (75% and 65%) results in Γ_{e_hh} of ~60.31%. By engineering the Al contents of the AlGaN layers as $x_1 = 0.75$ and $x_2 = 0.85$ [see Fig. 3(b)], the electron and hole wavefunctions are pushed toward the center of the QW active region, as the band gap of $Al_{0.85}Ga_{0.15}N$ is larger than that of $Al_{0.75}Ga_{0.25}N$, which results in the improved $\Gamma_{e\_hh} \sim 78.83\%$. Therefore, the matrix element will be enhanced attributing to the improved Γ_{e_hh}, which will contribute to the optical gain by using the optimized asymmetric AlGaN-delta-GaN QW structures.

3. Optical Gain Characteristics of Asymmetric AlGaN-Delta-GaN QWs

Fig. 4(a) shows the TE-polarized optical gain spectra for 30-Å $A_{0.8}Ga_{0.2}N$/3-Å GaN QWs with $n_{2D} = 1.65 \times 10^{13}$ cm^{-2} at T = 300 K with varying d_1 thicknesses. For the asymmetric QW with

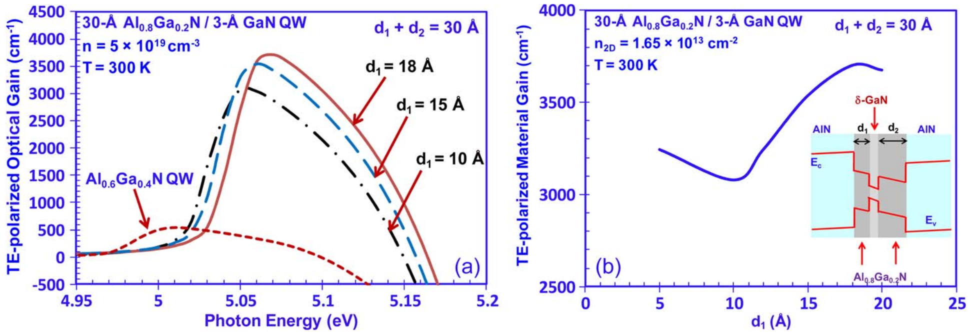

Fig. 4. (a) TE-polarized optical gain spectra for 30-Å $Al_{0.8}Ga_{0.2}N$/3-Å GaN QW with varying d_1 thicknesses, and (b) TE-polarized material peak gain as a function of the d_1 thickness for the 30-Å $Al_{0.8}Ga_{0.2}N$/3-Å GaN QW with $n_{2D} = 1.65 \times 10^{13}$ cm^{-2} at T = 300 K.

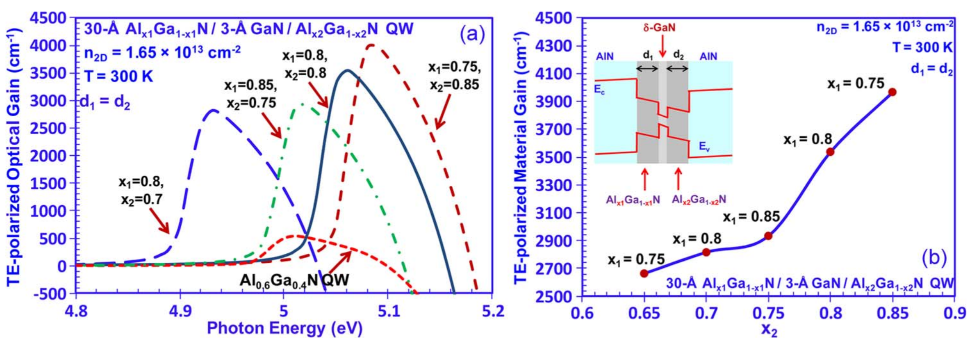

Fig. 5. (a) TE-polarized optical gain spectra for 30-Å $Al_{x1}Ga_{1-x1}N$/3-Å GaN/$Al_{x2}Ga_{1-x2}N$ QW with varying combinations of the Al contents x_1 and x_2, and (b) TE-polarized material peak gain for the 30-Å $Al_{x1}Ga_{1-x1}N$/3-Å GaN/$Al_{x2}Ga_{1-x2}N$ QW with $n_{2D} = 1.65 \times 10^{13}$ cm^{-2} at T = 300 K.

$d_1 = 18$ Å, the TE-polarized optical gain is larger than that of the symmetric QW with $d_1 = 15$ Å, attributing to the enhanced Γ_{e_hh} from the optimized AlGaN-delta-GaN QW structure. For the asymmetric QW with $d_1 = 10$ Å, the optical gain is slightly lower due to the weaker confinement of the electron and hole wavefunctions. Note that the peak emission wavelengths (λ_{peak}) for the asymmetric QWs with $d_1 = 10$ Å and 18 Å are ~246 nm and ~245 nm, respectively, which are very similar with that of the symmetric QW. In comparison with the conventional $Al_{0.6}Ga_{0.4}N$ QW, the optimized asymmetric delta QW ($d_1 = 18$ Å) shows ~6 times enhancement in the TE-polarized optical gain for mid-UV spectral regime.

Fig. 4(b) shows the TE-polarized material peak gain (g_{peak}^{TE}) as a function of the d_1 thickness for the 30-Å $Al_{0.8}Ga_{0.2}N$/3-Å GaN QW with $n_{2D} = 1.65 \times 10^{13}$ cm^{-2} at T = 300 K. With the d_1 thicknesses ranging from 5 Å up to 20 Å, the TE-polarized material gain varies from ~3078 cm^{-1} ($d_1 = 10$ Å) up to ~3703 cm^{-1} ($d_1 = 18$ Å). Therefore, very large optical gain can be maintained for emission wavelength ~245 nm for the asymmetric AlGaN-delta-GaN QW structures with different delta-GaN positions.

Fig. 5(a) illustrates the TE-polarized gain spectra for 30-Å $Al_{x1}Ga_{1-x1}N$/3-Å GaN/$Al_{x2}Ga_{1-x2}N$ QW with $n_{2D} = 1.65 \times 10^{13}$ cm^{-2} at T = 300 K with combinations x_1 and x_2. For the optimized delta QW with Al contents of $x_1 = 0.75$ and $x_2 = 0.85$, very large TE-polarized gain ($g_{peak}^{TE} \sim 3967$ cm^{-1}) can be obtained at $\lambda_{peak} \sim 244$ nm, attributed to the improved Γ_{e_hh} from the asymmetric QW. For the asymmetric cases of $Al_{0.85}Ga_{0.15}N$/3-Å GaN/$Al_{0.75}Ga_{0.25}N$ QW ($x_1 = 0.85, x_2 = 0.75$) and $Al_{0.8}Ga_{0.2}N$/3-Å GaN/$Al_{0.7}Ga_{0.3}N$ QW ($x_1 = 0.8, x_2 = 0.7$), large optical gains can be obtained with $\lambda \sim 244-252$ nm, which are ~6–7 times larger than that of the conventional QW emitting at similar wavelengths.

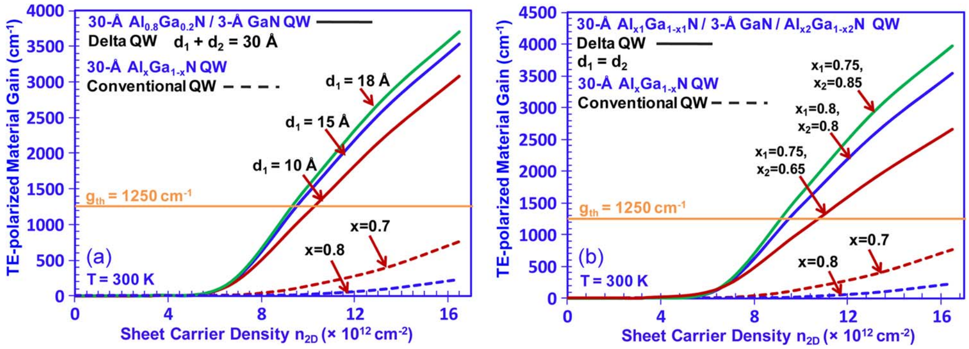

Fig. 6. TE-polarized material gain as a function of sheet carrier density for (a) 30-Å $Al_{0.8}Ga_{0.2}N$/3-Å GaN QW with varying d_1 thicknesses, and (b) 30-Å $A_{x1}Ga_{1-x1}N$/3-Å GaN/$Al_{x2}Ga_{1-x2}N$ QWs, in comparison with conventional 30-Å $Al_xGa_{1-x}N$ QW $(x = 0.7, 0.8)$.

Fig. 5(b) shows the TE-polarized material peak gain for the 30-Å $Al_{x1}Ga_{1-x1}N$/3-Å GaN/$Al_{x2}Ga_{1-x2}N$ QW with $n_{2D} = 1.65 \times 10^{13}$ cm^{-2} at T = 300 K. By varying the Al contents of the AlGaN layers surrounding the delta-GaN layer, the TE-polarized material peak gains range from $\sim$2700 cm^{-1} up to $\sim$4000 cm^{-1}. Therefore, the optimized asymmetric QW structures with different Al contents can lead to enhanced optical gain. Also, large TE-polarized gain can be maintained by different combinations of the Al contents of the AlGaN QWs, which will provide flexibility in the experimental realizations of the AlGaN-delta-GaN QWs mid- and deep-UV lasers.

4. Threshold Properties and Differential Gains of AlGaN-Delta-GaN QWs

Fig. 6(a) shows the TE-polarized material gain as a function of sheet carrier density for both 30-Å $Al_{0.8}Ga_{0.2}N$/3-Å GaN QWs with various d_1 thicknesses, and conventional 30-Å $Al_xGa_{1-x}N$ QW $(x = 0.7, 0.8)$ at T = 300 K. The g_{peak}^{TE} values of the AlGaN-delta-GaN QW structure $(\sim 3100-3700$ cm$^{-1})$ are found to be significantly larger than that of the conventional high Al-content AlGaN QWs $(\sim 200-800$ cm$^{-1})$ at high $n_{2D} = 1.65 \times 10^{13}$ cm^{-2}. The optimized asymmetric QW structure with $d_1 = 18$ Å achieves $\sim$1.2 times larger material gain than that of the symmetric QW structure, attributing to its improved matrix element.

To illustrate the effect of different Al contents of the AlGaN QWs, Fig. 6(b) shows the TE-polarized material gain as a function of sheet carrier density for 30-Å $Al_{x1}Ga_{1-x1}N$/3-Å GaN/$Al_{x2}Ga_{1-x2}N$ QWs and conventional 30-Å $Al_xGa_{1-x}N$ QWs $(x = 0.7, 0.8)$ at T = 300 K. Attributing to the reduced charge separation effect, the optimized asymmetric 30-Å $Al_{0.75}Ga_{0.25}N$/3-Å GaN/$Al_{0.85}Ga_{0.15}N$ QW achieves $\sim$1.4 times larger material gain than that of the symmetric QW. Thus, the TE-polarized lasing is feasible for asymmetric AlGaN-delta-GaN QW lasers with $\lambda \sim 240-250$ nm.

To analyze the threshold properties of mid- and deep-UV lasers, AlGaN QW lasers with optical confinement factor (Γ_{opt}) of 0.02 [41] were used in the analysis. Based on the transfer matrix method [64], the Γ_{opt} for the asymmetric and symmetric QWs are calculated as almost identical. Thus, the modal gain comparison for the QWs will be governed by the difference in the material gains. The internal loss (α_i) in typical AlGaN lasers is 14 cm^{-1} [35]. The laser cavity length is assumed as 500 μm [35], [41] with end-facet reflectivities of 95% and 35%, which corresponds to mirror loss (α_m) of 11 cm^{-1} and threshold gain (g_{th}) of $\sim$1250 cm^{-1}. The threshold sheet carrier density (n_{2D}^{th}) is 9.273×10^{12} cm^{-2} for the symmetric 30-Å $Al_{0.8}Ga_{0.2}N$/3-Å GaN QW. For the optimized structure with $d_1 = 18$ Å [see Fig. 6(a)], the n_{2D}^{th} is 9.042×10^{12} cm^{-2}. Similarly, for optimized 30-Å $Al_{0.75}Ga_{0.25}N$/3-Å GaN/$Al_{0.85}Ga_{0.15}N$ QW, the n_{2D}^{th} is 8.976×10^{12} cm^{-2}. Thus, the n_{2D}^{th} for both optimized AlGaN-delta-GaN QW structures with different delta-GaN positions and varying Al contents are reduced compared with the symmetric QW.

The spontaneous emission rates and peak modal gains (with $\Gamma_{opt} = 0.02$ [41]) comparisons for both symmetric and asymmetric AlGaN-Delta-GaN QWs are presented in Figs. 7 and 8, respectively. The comparison studies were performed for AlGaN-Delta-GaN QWs with different delta layer

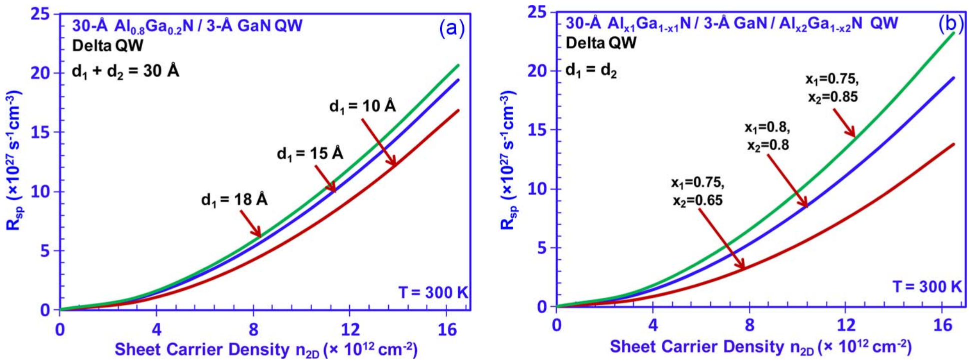

Fig. 7. R_{sp} as a function of sheet carrier density for both symmetric and asymmetric AlGaN-Delta-GaN QWs to illustrate (a) effect of delta positions, and (b) effect of Al contents in AlGaN QWs.

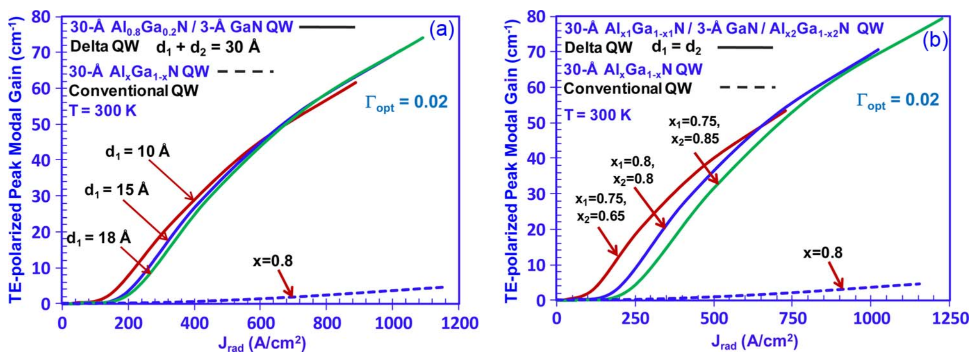

Fig. 8. Modal gains as a function of radiative current density for AlGaN-Delta-GaN QWs and conventional $Al_{0.8}Ga_{0.2}N$ QW with different (a) delta positions, and (b) Al contents in AlGaN QWs.

position (d_1, d_2) [see Figs. 7(a) and 8(a)] and different AlGaN QW sublayer compositions [see Figs. 7(b) and 8(b)]. By comparing the R_{sp} for different delta-layer positions [see Fig. 7(a)], the asymmetric delta QW with $d_1 = 18$ Å shows higher R_{sp} ($\sim 2.07 \times 10^{28}$ $s^{-1}cm^{-3}$ with $n_{2D} = 1.65 \times 10^{13}$ cm^{-2}) than those of the other structures, attributed from the improved overlap $(\Gamma_{e\_hh} \sim 73.92\%)$. Fig. 7(b) shows that the optimized R_{sp} was obtained from the use of that for $Al_{0.75}Ga_{0.25}N$/3-Å GaN/$Al_{0.85}Ga_{0.15}N$ QWs attributed to the optimized C–HH overlap of 78.83%. The delta QWs exhibited significantly higher modal gain for any radiative current density (J_{rad}) injection level [see Fig. 8(a) and (b)], in comparison with those the conventional QW. The total recombination current density J_{tot} in the QW active region includes both the radiative and nonradiative current densities $(J_{tot} = J_{rad} + J_{non-rad})$ [58], and $J_{non-rad}$ $(\sim A \cdot n_{th} + C \cdot n_{th}^3)$ represents the dominant part of the J_{tot} in AlGaN-based QW [41], [58]. Thus, the reduction in n_{th} is important for suppressing monomolecular $(\sim A \cdot n_{th})$ and Auger $(\sim C \cdot n_{th}^3)$ recombination currents at threshold.

The differential gain properties are also analyzed for both symmetric and asymmetric AlGaN-Delta-GaN QWs to illustrate effect of delta positions [see Fig. 9(a)], as well as effect of Al contents [see Fig. 9(b)]. For both cases, the differential gains first increase with higher carrier densities, which can be attributed to the carrier screening effect. After reaching the maximum, the differential gains start to decrease with increasing carrier densities, which is due to the band filling effect. In Fig. 9(a) and (b), the peak differential gains of the optimized asymmetric AlGaN-delta-GaN QW structures are higher than those of the symmetric QW structures, which indicates that the optimized AlGaN-delta-GaN QW structures will be applicable for high-speed modulation lasers.

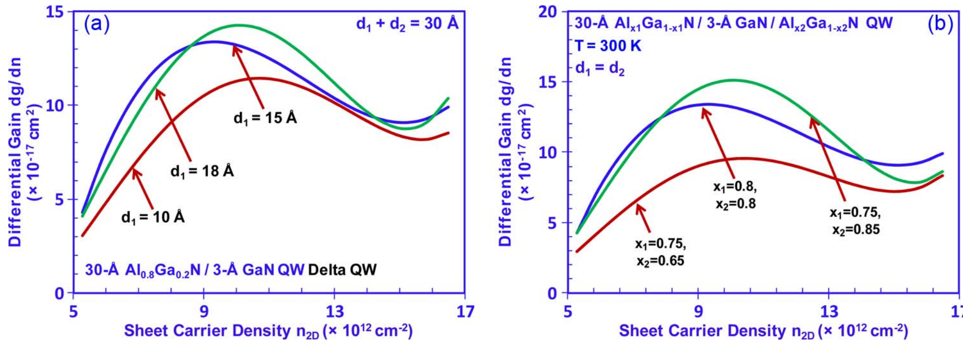

Fig. 9. Differential gain as a function of sheet carrier density for AlGaN-Delta-GaN QWs to illustrate the effect of (a) delta positions, and (b) Al contents of AlGaN QWs

5. Summary

In summary, the comprehensive optimization studies on the gain characteristics of AlGaN-delta-GaN QWs with various delta-GaN positions and AlGaN compositions are analyzed. The optimized asymmetric AlGaN-delta-GaN QWs result in $\sim$7 times increase in material gain, in comparison with that of the conventional QWs. Recent works had reported the TE-polarized gain from the following: 1) $Al_{0.7}Ga_{0.3}N$/AlN QWs with low Al-content nanocluster "quantum dot" features within the $Al_{0.7}Ga_{0.3}N$ QW layers [65], [66] and 2) thin GaN "quantum dot" structures embedded in AlN barriers [67], which are consistent with the dominant TE-polarized gain from our prediction for high Al-content AlGaN QWs consisting of low band-gap GaN delta layer embedded in the active region [51]. Large material gains can be maintained at $\lambda \sim 240-250$ nm for the asymmetric AlGaN-delta-GaN QWs [see Fig. 4(b)]. Despite the improved material gain for the asymmetric QWs, the finding shows that large material gain can be obtained for both symmetric and asymmetric AlGaN-delta-GaN QWs [see Fig. 4(b)], which indicates the flexibility and robustness in the experimental implementations of this concept in devices. Thus, by employing asymmetric QW design with optimized delta-GaN layer position and asymmetric AlGaN-composition layers, the optimized optical gain and lower threshold carrier densities are achievable for the AlGaN-delta-GaN QW with realistic design applicable for mid- and deep-UV lasers. Recent works by metalorganic chemical vapor deposition (MOCVD) had reported the growths of AlN/ GaN superlattice structures with thin GaN layers in the order of $\sim$0.9–2.5 monolayers [52]. Thus, the growths of the AlGaN-delta-GaN QW is expected to be practical for implementation in deep/mid-UV LEDs or lasers.

References

[1] R. M. Farrell, E. C. Young, F. Wu, S. P. DenBaars, and J. S. Speck, "Materials and growth issues for high-performance nonpolar and semipolar light-emitting devices," *Semicond. Sci. Technol.*, vol. 27, no. 2, p. 024001, Feb. 2012.

[2] H. P. Zhao, G. Y. Liu, J. Zhang, J. D. Poplawsky, V. Dierolf, and N. Tansu, "Approaches for high internal quantum efficiency green InGaN light-emitting diodes with large overlap quantum wells," *Opt. Exp.*, vol. 19, no. S4, pp. A991–A1007, Jul. 2011.

[3] J. H. Ryou, P. D. Yoder, J. P. Liu, Z. Lochner, H. Kim, S. Choi, H. J. Kim, and R. D. Dupuis, "Control of quantum-confined stark effect in InGaN-based quantum wells," *IEEE J. Sel. Topics Quantum Electron.*, vol. 15, no. 4, pp. 1080–1091, Jul./Aug. 2009.

[4] I. H. Brown, P. Blood, P. M. Smowton, J. D. Thomson, S. M. Olaizola, A. M. Fox, P. J. Parbrook, and W. W. Chow, "Time evolution of the screening of piezoelectric fields in InGaN quantum wells," *IEEE J. Quantum Electron.*, vol. 42, no. 12, pp. 1202–1208, Dec. 2006.

[5] Y. K. Ee, J. M. Biser, W. Cao, H. M. Chan, R. P. Vinci, and N. Tansu, "Metalorganic vapor phase epitaxy of III-nitride light-emitting diodes on nanopatterned AGOG sapphire substrate by abbreviated growth mode," *IEEE J. Sel. Topics Quantum Electron.*, vol. 15, no. 4, pp. 1066–1072, Jul./Aug. 2009.

[6] Y. Li, S. You, M. Zhu, L. Zhao, W. Hou, T. Detchprohm, Y. Taniguchi, N. Tamura, S. Tanaka, and C. Wetzel, "Defect-reduced green GaInN/GaN light-emitting diode on nanopatterned sapphire," *Appl. Phys. Lett.*, vol. 98, no. 15, pp. 151102-1–151102-3, Apr. 2011.

[7] X. Li, S. Kim, E. E. Reuter, S. G. Bishop, and J. J. Coleman, "The incorporation of arsenic in GaN by metalorganic chemical vapor deposition," *Appl. Phys. Lett.*, vol. 72, no. 16, pp. 1990–1992, Apr. 1998.

[8] T. Jung, L. K. Lee, and P.-C. Ku, "Novel epitaxial nanostructures for the improvement of InGaN LEDs efficiency," *IEEE J. Sel. Topics Quantum Electron.*, vol. 15, no. 4, pp. 1073–1079, Jul./Aug. 2009.
[9] X. Li, S. G. Bishop, and J. J. Coleman, "GaN epitaxial lateral overgrowth and optical characterization," *Appl. Phys. Lett.*, vol. 73, no. 9, pp. 1179–1181, Aug. 1998.
[10] W. Guo, A. Banerjee, P. Bhattacharya, and B. S. Ooi, "InGaN/GaN disk-in-nanowire white light emitting diodes on (001) silicon," *Appl. Phys. Lett.*, vol. 98, no. 19, pp. 193102-1–193102-3, May 2011.
[11] X. H. Li, R. B. Song, Y. K. Ee, P. Kumnorkaew, J. F. Gilchrist, and N. Tansu, "Light extraction efficiency and radiation patterns of III-nitride light-emitting diodes with colloidal microlens arrays with various aspect ratios," *IEEE Photon. J.*, vol. 3, no. 3, pp. 489–499, Jun. 2011.
[12] J. Jewell, D. Simeonov, S.-C. Huang, Y.-L. Hu, S. Nakamura, J. Speck, and C. Weisbuch, "Double embedded photonic crystals for extraction of guided light in light-emitting diodes," *Appl. Phys. Lett.*, vol. 100, no. 17, p. 171105, Apr. 2012.
[13] M. H. Kim, M. F. Schubert, Q. Dai, J. K. Kim, E. F. Schubert, J. Piprek, and Y. Park, "Origin of efficiency droop in GaN-based light-emitting diodes," *Appl. Phys. Lett.*, vol. 91, no. 18, pp. 183507-1–183507-3, Oct. 2007.
[14] H. Zhao, G. Liu, R. A. Arif, and N. Tansu, "Current injection efficiency induced efficiency-droop in InGaN quantum well light-emitting diodes," *Solid State Electron.*, vol. 54, no. 10, pp. 1119–1124, Oct. 2010.
[15] C. H. Wang, C. C. Ke, C. Y. Lee, S. P. Chang, W. T. Chang, J. C. Li, Z. Y. Li, H. C. Yang, H. C. Kuo, T. C. Lu, and S. C. Wang, "Hole injection and efficiency droop improvement in InGaN/GaN light-emitting diodes by band-engineered electron blocking layer," *Appl. Phys. Lett.*, vol. 9726, pp. 261103-1–261103-3, Dec. 2010.
[16] J. Piprek, "Efficiency droop in nitride-based light-emitting diodes," *Phys. Stat. Sol. (A), Appl. Mater. Sci.*, vol. 207, no. 10, pp. 2217–2225, Oct. 2010.
[17] U. K. Mishra, P. Parikh, and Y. F. Wu, "AlGaN/GaN HEMTs-an overview of device operation and applications," *Proc. IEEE*, vol. 90, no. 6, pp. 1022–1031, Jun. 2002.
[18] B. N. Pantha, R. Dahal, J. Li, J. Y. Lin, H. X. Jiang, and G. Pomrenke, "Thermoelectric properties of $In_xGa_{1-x}N$ alloys," *Appl. Phys. Lett.*, vol. 92, no. 4, pp. 042112-1–042112-3, Jan. 2008.
[19] J. Zhang, S. Kutlu, G. Y. Liu, and N. Tansu, "High-temperature characteristics of seebeck coefficients for AlInN alloys grown by metalorganic vapor phase epitaxy," *J. Appl. Phys.*, vol. 110, no. 4, p. 043710, Aug. 2011.
[20] B. N. Pantha, I.-W. Feng, K. Aryal, J. Li, J.-Y. Lin, and H.-X. Jiang, "Erbium-doped AlInGaN alloys as high-temperature thermoelectric materials," *Appl. Phys. Exp.*, vol. 4, no. 5, pp. 051001-1–051001-3, May 2011.
[21] G. Sun, G. Xu, Y. J. Ding, H. P. Zhao, G. Y. Liu, J. Zhang, and N. Tansu, "Efficient terahertz generation from multiple InGaN/GaN quantum wells," *IEEE J. Sel. Topics Quantum Electron.*, vol. 17, no. 1, pp. 48–53, Jan./Feb. 2011.
[22] A. Yasan, R. McClintock, K. Mayes, D. Shiell, L. Gautero, S. R. Darvish, P. Kung, and M. Razeghi, "4.5 mW operation of AlGaN-based 267 nm deep-ultraviolet light-emitting diodes," *Appl. Phys. Lett.*, vol. 83, no. 23, pp. 4701–4703, Dec. 2003.
[23] A. J. Fischer, A. A. Allerman, M. H. Crawford, K. H. A. Bogart, S. R. Lee, R. J. Kaplar, W. W. Chow, S. R. Kurtz, K. W. Fullmer, and J. J. Figiel, "Room-temperature direct current operation of 290 nm light-emitting diodes with milliwatt power levels," *Appl. Phys. Lett.*, vol. 84, no. 17, pp. 3394–3396, Apr. 2004.
[24] V. Adivarahan, S. Wu, J. P. Zhang, A. Chitnis, M. Shatalov, V. Mandavilli, R. Gaska, and M. A. Khan, "High-efficiency 269 nm emission deep ultraviolet light-emitting diodes," *Appl. Phys. Lett.*, vol. 84, no. 23, pp. 4762–4764, Jun. 2004.
[25] Z. Ren, Q. Sun, S. Y. Kwon, J. Han, K. Davitt, Y. K. Song, A. V. Nurmikko, H.-K. Cho, W. Liu, J. A. Smart, and L. J. Schowalter, "Heteroepitaxy of AlGaN on bulk AlN substrates for deep ultraviolet light emitting diodes," *Appl. Phys. Lett.*, vol. 91, no. 5, pp. 051116-1–051116-3, Jul. 2007.
[26] A. V. Sampath, M. L. Reed, C. Chua, G. A. Garrett, G. Dang, E. D. Readinger, H. Shen, A. Usikov, O. Kovalenkov, L. Shapovalova, V. A. Dmitriev, N. M. Johnson, and M. Wraback, "Double heterostructure ultraviolet light emitting diodes with nanometer scale compositionally inhomogeneous active regions," *Phys. Stat. Sol. (C)*, vol. 5, no. 6, pp. 2303–2305, Apr. 2008.
[27] C. G. Moe, M. L. Reed, G. A. Garrett, A. V. Sampath, T. Alexander, H. Shen, M. Wraback, Y. Bilenko, M. Shatalov, J. Yang, W. Sun, J. Deng, and R. Gaska, "Current-induced degradation of high performance deep ultraviolet light emitting diodes," *Appl. Phys. Lett.*, vol. 96, no. 21, pp. 213512-1–213512-3, May 2010.
[28] Y. Sakai, Y. Zhu, S. Sumiya, M. Miyoshi, M. Tanaka, and T. Egawa, "Demonstration of AlGaN-based deep-ultraviolet light-emitting diodes on high-quality AlN templates," *Jpn. J. Appl. Phys.*, vol. 49, no. 2, p. 022102, Feb. 2010.
[29] Y. Taniyasu and M. Kasu, "Surface 210 nm light emission from an AlN p–n junction light-emitting diode enhanced by A-plane growth orientation," *Appl. Phys. Lett.*, vol. 96, no. 22, pp. 221110-1–221110-1, May 2010.
[30] H. Hirayama, N. Noguchi, and N. Kamata, "222 nm Deep-ultraviolet AlGaN quantum well light-emitting diode with vertical emission properties," *Appl. Phys. Exp.*, vol. 3, no. 3, pp. 032102-1–032102-3, Mar. 2010.
[31] T. Takano, Y. Narita, A. Horiuchi, and H. Kawanishi, "Room-temperature deep-ultraviolet lasing at 241.5 nm of AlGaN multiple-quantum-well laser," *Appl. Phys. Lett.*, vol. 84, no. 18, pp. 3567–3569, May 2004.
[32] M. Kneissl, Z. Yang, M. Teepe, C. Knollenberg, O. Schmidt, P. Kiesel, N. M. Johnson, S. Schujman, and L. J. Schowalter, "Ultraviolet semiconductor laser diodes on bulk AlN," *J. Appl. Phys.*, vol. 101, no. 12, p. 123103, Jun. 2007.
[33] V. N. Jmerik, A. M. Mizerov, A. A. Sitnikova, P. S. Kopev, S. V. Ivanov, E. V. Lutsenko, N. P. Tarasuk, N. V. Rzheutskii, and G. P. Yablonskii, "Low-threshold 303 nm lasing in AlGaN-based multiple-quantum well structures with an asymmetric waveguide grown by plasma-assisted molecular beam epitaxy on c-sapphire," *Appl. Phys. Lett.*, vol. 96, no. 14, pp. 141112-1–141112-3, Apr. 2010.
[34] H. Yoshida, M. Kuwabara, Y. Yamashita, K. Uchiyama, and H. Kan, "Radiative and nonradiative recombination in an ultraviolet GaN/AlGaN multiple-quantum-well laser diode," *Appl. Phys. Lett.*, vol. 96, no. 21, p. 211122, May 2010.
[35] H. Yoshida, M. Kuwabara, Y. Yamashita, Y. Takagi, K. Uchiyama, and H. Kan, "AlGaN-based laser diodes for the short-wavelength ultraviolet region," *New J. Phys.*, vol. 11, no. 12, p. 125013, Dec. 2009.
[36] M. Kneissl, D. W. Treat, M. Teepe, N. Miyashita, and N. M. Johnson, "Continuous-wave operation of ultraviolet InGaN/InAlGaN multiple-quantum-well laser diodes," *Appl. Phys. Lett.*, vol. 82, no. 15, pp. 2386–2388, Apr. 2003.

[37] C. Chen, M. Shatalov, E. Kuokstis, V. Adivarahan, M. Gaevski, S. Rai, and M. Asif Khan, "Optically pumped lasing at 353 nm using non-polar a-plane AlGaN multiple quantum wells over r-plane sapphire," *Jpn. J. Appl. Phys.*, vol. 43, no. 8B, pp. L1 099–L1 102, Jul. 2004.
[38] D. A. Haeger, E. C. Young, R. B. Chung, F. Wu, N. A. Pfaff, M. Tsai, K. Fujito, S. P. DenBaars, J. S. Speck, S. Nakamura, and D. A. Cohen, "384 nm Laser diode grown on a (2021) semipolar relaxed AlGaN buffer layer," *Appl. Phys. Lett.*, vol. 100, no. 16, pp. 161107-1–161107-4, Apr. 2012.
[39] C. P. Wang and Y. R. Wu, "Study of optical anisotropy in nonpolar and semipolar AlGaN quantum well deep ultraviolet light emission diode," *J. Appl. Phys.*, vol. 112, no. 3, pp. 033104-1–033104-7, Aug. 2012.
[40] W. W. Chow, M. Kneissl, J. E. Northrup, and N. M. Johnson, "Influence of quantum-well-barrier composition on gain and threshold current in AlGaN lasers," *Appl. Phys. Lett.*, vol. 90, no. 10, pp. 101116-1–101116-3, Mar. 2007.
[41] W. W. Chow and M. Kneissl, "Laser gain properties of AlGaN quantum wells," *J. Appl. Phys.*, vol. 98, no. 11, pp. 114502-1–114502-6, Dec. 2005.
[42] S. H. Park and S. L. Chuang, "Linewidth enhancement factor of wurtzite GaN/AlGaN quantum-well lasers with spontaneous polarization and piezoelectric effects," *Appl. Phys. A*, vol. 78, no. 1, pp. 107–111, Jan. 2004.
[43] J. Zhang, H. Zhao, and N. Tansu, "Effect of crystal-field split-off hole and heavy-hole bands crossover on gain characteristics of high Al-content AlGaN quantum well lasers," *Appl. Phys. Lett.*, vol. 97, no. 11, p. 111105, Sep. 2010.
[44] S. H. Park, "Theoretical study of optical properties in deep ultraviolet Al-rich AlGaN/AlN quantum wells," *Semicond. Sci. Technol.*, vol. 24, no. 3, p. 035002, Mar. 2009.
[45] T. Kolbe, A. Knauer, C. Chua, Z. Yang, S. Einfeldt, P. Vogt, N. M. Johnson, M. Weyers, and M. Kneissl, "Optical polarization characteristics of ultraviolet (In)(Al)GaN multiple quantum well light emitting diodes," *Appl. Phys. Lett.*, vol. 97, no. 17, pp. 171105-1–171105-3, Oct. 2010.
[46] T. M. Al tahtamouni, J. Y. Lin, and H. X. Jiang, "Optical polarization in c-plane Al-rich AlN/$Al_xGa_{1-x}N$ single quantum wells," *Appl. Phys. Lett.*, vol. 101, no. 4, pp. 042103-1–042103-3, Jul. 2012.
[47] T. Kolbe, A. Knauer, C. Chua, Z. Yang, V. Kueller, S. Einfeldt, P. Vogt, N. M. Johnson, M. Weyers, and M. Kneissl, "Effect of temperature and strain on the optical polarization of (In)(Al)GaN ultraviolet light emitting diodes," *Appl. Phys. Lett.*, vol. 99, no. 26, pp. 261105-1–261105-4, Dec. 2011.
[48] T. K. Sharma and E. Towe, "Impact of strain on deep ultraviolet nitride laser and light-emitting diodes," *J. Appl. Phys.*, vol. 109, no. 8, pp. 086104-1–086104-3, Apr. 2011.
[49] T. K. Sharma, D. Naveh, and E. Towe, "Strain-driven light-polarization switching in deep ultraviolet nitride emitters," *Phys. Rev. B*, vol. 84, no. 3, pp. 035305-1–035305-8, Jul. 2011.
[50] G. A. Garrett, P. Rotella, H. Shen, M. Wraback, T. Wunderer, C. L. Chua, Z. Yang, J. E. Northrup, and N. M. Johnson, "Sub-threshold time-resolved spectroscopy of mid-UV AlGaN laser diode structures pseudomorphically grown on bulk AlN," presented at the IEEE/OSA Conf. Lasers and Electro-Optics (CLEO), San Jose, CA, USA, 2012, Paper JTh1L.5.
[51] J. Zhang, H. Zhao, and N. Tansu, "Large optical gain AlGaN-delta-GaN quantum wells laser active regions in mid- and deep-ultraviolet spectral regimes," *Appl. Phys. Lett.*, vol. 98, no. 17, pp. 171111-1–171111-3, Apr. 2011.
[52] Y. Taniyasu and M. Kasu, "Polarization property of deep-ultraviolet light emission from C-plane AlN/GaN short-period superlattices," *Appl. Phys. Lett.*, vol. 99, no. 25, pp. 251112-1–251112-4, Dec. 2011.
[53] H. Zhao, G. Liu, and N. Tansu, "Analysis of InGaN-Delta-InN quantum wells for light-emitting diodes," *Appl. Phys. Lett.*, vol. 97, no. 13, pp. 131114-1–131114-3, Sep. 2010.
[54] H. Zhao, X. Jiao, and N. Tansu, "Analysis of position and thickness dependences of delta layer in InGaN-Delta-InN quantum wells light-emitting diodes," in *Asia Communications Photonics Conf. (ACP)*, Guangzhou, China, Nov. 2012.
[55] S. L. Chuang, "Optical gain of strained wurtzite GaN quantum-well lasers," *IEEE J. Quantum Electron.*, vol. 32, no. 10, pp. 1791–1800, Oct. 1996.
[56] S. L. Chuang and C. S. Chang, "A band-structure model of strained quantum-well wurtzite semiconductors," *Semicond. Sci. Technol.*, vol. 12, no. 3, pp. 252–263, Mar. 1997.
[57] S. L. Chuang, *Physics of Photonic Devices*, 2nd ed. New York, NY, USA: Wiley, 2009.
[58] H. Zhao, R. A. Arif, Y. K. Ee, and N. Tansu, "Self-consistent analysis of strain-compensated InGaN–AlGaN quantum wells for lasers and light-emitting diodes," *IEEE J. Quantum Electron.*, vol. 45, no. 1, pp. 66–78, Jan. 2009.
[59] H. Zhao and N. Tansu, "Optical gain characteristics of staggered InGaN quantum wells lasers," *J. Appl. Phys.*, vol. 107, no. 11, pp. 113110-1–113110-12, Jun. 2010.
[60] I. Vurgaftman and J. R. Meyer, *Chapter 2 in Nitride Semiconductor Devices*, J. Piprek, Ed. Hoboken, NJ, USA: Wiley, 2007.
[61] I. Vurgaftman and J. R. Meyer, "Band parameters for nitrogen-containing semiconductors," *J. Appl. Phys.*, vol. 94, no. 6, pp. 3675–3696, Sep. 2003.
[62] F. Bernardini and V. Fiorentini, "Spontaneous versus piezoelectric polarization in III–V Nitrides: Conceptual aspects and practical consequences," *Phys. Stat. Sol. (B)*, vol. 216, no. 1, pp. 391–398, Nov. 1999.
[63] O. Ambacher, J. Majewski, C. Miskys, A. Link, M. Hermann, M. Eickhoff, M. Stutzmann, F. Bernardini, V. Fiorentini, V. Tilak, B. Schaff, and L. F. Eastman, "Pyroelectric properties of Al(In)GaN/GaN hetero and quantum well structures," *J. Phys., Condens. Matter*, vol. 14, pp. 3399–3434, Apr. 2002.
[64] P. Yeh, *Optical Waves in Layered Media*. New York, NY, USA: Wiley, 2005.
[65] E. F. Pecora, W. Zhang, A. Y. Nikiforov, L. Zhou, D. J. Smith, J. Yin, R. Paiella, L. D. Negro, and T. D. Moustakas, "Sub-250 nm room-temperature optical gain from AlGaN/AlN multiple quantum wells with strong band-structure potential fluctuations," *Appl. Phys. Lett.*, vol. 100, no. 6, pp. 061111-1–061111-4, Feb. 2012.
[66] E. F. Pecora, W. Zhang, J. Yin, R. Paiella, L. D. Negro, and T. D. Moustakas, "Polarization properties of deep-ultraviolet optical gain in Al-rich AlGaN structures," *Appl. Phys. Exp.*, vol. 5, no. 3, pp. 032103-1–032103-3, Mar. 2012.
[67] J. Verma, P. Kandaswamy, V. Protasenko, A. Verma, H. Xing, and D. Jena, "Tunnel-injection GaN quantum dot ultraviolet light-emitting diodes," *Appl. Phys. Lett.*, vol. 102, no. 4, pp. 041103-1–041103-4, Jan. 2013.